Liquid-Phase Polymerization of Propylene with a Highly Active Ziegler–Natta Catalyst. Influence of Hydrogen, Cocatalyst, and Electron Donor on the Reaction Kinetics

JOB JAN C. SAMSON, PETER J. BOSMAN, GÜNTER WEICKERT, K. ROEL WESTERTERP

Chemical Reaction Engineering Laboratories, Department of Chemical Engineering, Twente University of Technology, P.O. Box 217, 7500 AE Enschede, The Netherlands

ABSTRACT: This paper presents an experimental kinetic study of the polymerization of propylene in liquid monomer with a high activity catalyst. The influences of the concentration of hydrogen and the molar ratios of the catalyst, cocatalyst, and electron donor on the activation period, the maximum activity, the yield, and the decay behavior have been investigated at a temperature of 42°C using a relatively simple kinetic model. On the basis of the experimental data, the reaction rate has been modeled as a function of the hydrogen concentration, the molar ratio of cocatalyst and titanium, and the molar ratio of the electron donor and the cocatalyst. © 1999 John Wiley & Sons, Inc. J Polym Sci A: Polym Chem 37: 219–232, 1999

Keywords: catalytic polymerization; Ziegler–Natta catalyst; reaction kinetics; propylene polymerization; liquid pool

INTRODUCTION

Despite the fact that most commercial polypropylene polymerizations are carried out either in liquid or gaseous monomer, only a few papers provide kinetic data gathered from experiments in liquid or gaseous propylene. In this paper, we describe an investigation of the polymerization of propylene with a high activity catalyst under industrial reaction conditions to provide kinetic data and to obtain a better understanding of the polymerization process. Further, we demonstrate the suitability of small-scale liquid pool experiments to determine kinetics. In liquid pool experiments no solvent like heptane is used and the reaction is executed in pure propylene. Limitations in the mass transfer of gaseous monomer to the solvent as often encountered in slurry polymerizations are absent.

In our experimental program, we have used a highly active $MgCl_2/TiCl_4$ catalyst, suitable for liquid pool and gas phase polymerizations. The catalyst contains ethyl benzoate (EB) as the internal electron donor and has been used in conjunction with ethyl p-ethoxybenzoate (PEEB) as the external electron donor and triethylaluminum (TEAl) as the cocatalyst. In a series of experiments, the influence of the polymerization conditions on the reaction kinetics of the propylene polymerization in liquid monomer has been studied. We have varied from 0.0 to 12 vol. % the concentration of hydrogen in the gas cap of the reactor and from 100 to 900 the molar ratio of cocatalyst and Ti; the molar ratio of electron donor and cocatalyst has been varied from 0.0 to 4.0. The experimental results have been used to investigate the influence of the before mentioned parameters on the yield, initial reaction rate, decay rate, and induction period, respectively.

The used catalyst may not belong to the latest catalysts, but today the greatest part of polypropylene is still produced with $MgCl_2/TiCl_4$-based Ziegler–Natta catalysts. These catalysts are rela-

tively cheap and produce polymers with broad molecular weight distributions. These polymers are suitable for many applications due to their excellent mechanical properties and ease of processing. Therefore, likely a significant share of the polypropylene market will still be produced on the basis of the $MgCl_2/TiCl_4$ catalyst family for many years.

EXPERIMENTAL

The experimental setup for liquid pool polymerizations comprises a 5 L jacketed reactor, a special catalyst injection system, and further purification systems for propylene, hydrogen, nitrogen, and pentane and has been described in detail by Samson et al.[7] The experiments are executed batchwise under isothermal conditions. The heat transfer coefficient remains constant up to about 35% conversion. Thus, the reaction rate can be determined calorimetrically from the temperature difference between reaction mass and cooling water. During polymerization, the reactor temperature is controlled within 0.1°C from the setpoint. The experimental setup is automated to a great extent to simplify operation, safeguard safety, and enhance processing of the measured data.

We have chosen to execute this series of experiments at a relatively low temperature of 42°C to avoid too high initial reaction rates, i.e. above 50–100 kg/(g of catal. h), which may result in a particle runaway and as a consequence thermal deactivation of the catalyst.

Polymerization Procedure

To start a polymerization, the reactor is first cleaned intensively at 50°C during 1 h with a mixture of 1 L of liquid propylene and about 250 mg of DEAC to scavenge water, oxygen, and other impurities from the reactor wall. Then the liquid propylene/DEAC mixture is removed from the reactor through a drain at the bottom. Next, the reactor is filled with a prescribed amount of hydrogen and 2.6 L of fresh, liquid propylene for polymerization and heated to a temperature of 42°C. Catalyst, cocatalyst (TEAl), and external electron donor (PEEB) are separately weighed in small vials in a glovebox. The vials are sealed with a septum and transferred to the catalyst injection system. With intervals of 1 min the cocatalyst, electron donor, and $MgCl_2/TiCl_4/EB$ catalyst are injected in said order into the reactor.

From the moment the $MgCl_2/TiCl_4/EB$ catalyst is injected, the reaction starts and the temperatures of the reactor and coolant and the pressure are registered. After 75 min of reaction time a few milliliters of methanol are injected into the reactor to kill the catalyst. Finally, the remaining monomer is slowly vented and the polymer product removed from the reactor and vacuum dried at 50°C.

Kinetic Model

The kinetics are studied qualitatively and quantitatively on the basis of the kinetic model, which was proposed earlier.[7,8] Below, a short description of this model is given. The following relation describes the reaction rate:

$$R_p = k_p C_m C^* \qquad (1)$$

Here $k_p = k_{p,0}e^{-E_{a,p}/RT}$, where k_p is the propagation rate constant and $E_{a,p}$ the lumped activation energy for the propagation reactions. Further, C_m is the monomer concentration in the polymer and C^* is the number of active centers per gram of catalyst. The decay of the catalyst is described by the decrease in time of the number of active centers, according to the following equation:

$$-\frac{dC^*}{dt} = k_d(C^*)^n \qquad (2)$$

Here $k_d = k_{d,0}e^{-E_{a,d}/RT}$, where k_d is the deactivation constant, n is the order of deactivation, $E_{a,d}$ is the activation energy for the lumped deactivation reactions, and T is the temperature. Combination of the eqs. (1) and (2) gives

$$-\frac{dR_p}{dt} = K_D R_p^n \qquad (3)$$

with $K_D = (k_{d,0}/(k_{p,0}C_m)^{n-1}) e^{((n-1)E_{a,p} - E_{a,d})/RT}$.

Integration of eq. (3) gives the reaction rate as a function of time:

$$R_p = (R_{p,0}^{(1-n)} + (n-1)K_D t)^{1/1-n} \quad n \neq 1 \qquad (4)$$

with $R_{p,0} = k_{p,0}e^{-E_{a,p}/RT}C_m C_0^*$, where $R_{p,0}$ is the initial reaction rate and K_D a measure of the deactivation rate.
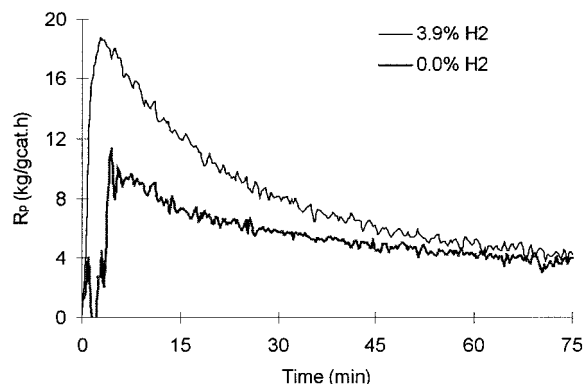
Figure 1. Typical experimental reaction rate curves for experiments executed with or without hydrogen in the gas cap.

RESULTS

Reproducibility

Propylene polymerizations with Ziegler–Natta catalysts are rather difficult to carry out because of the extreme purity required of the raw materials. For example, traces of H_2O, O_2, CO_2, and sulfur compounds rapidly kill the catalyst. The activity and decay behavior of the catalyst depend on the molar ratios between catalyst, TEAl, and PEEB and the concentration of hydrogen. In order to avoid variations in the composition of the raw materials, we have used one same batch of propylene, catalyst, TEAl, and PEEB. To check the catalyst activity, the purity of raw materials, and the condition of the equipment, a standard test was executed regularly. Throughout the series of experiments described in this paper, the yield of the standard test has been reproducible within 7%. In this paper, the reaction rates and yields are given per gram of $Mg_2Cl_4/TiCl_4/EB$ catalyst.

Influence of Process Conditions

The influence of hydrogen, cocatalyst, and electron donor on the catalyst activity and decay be-

havior has been studied by using the kinetic model described earlier in this paper. In the analyses of the experimental data, we have used eq. (4) with the constant order of deactivation of $n = 2$. At isothermal conditions, eq. (4) simplifies to eq. (5),

$$R_p = (R_{p,0}^{(1-n)} + (n-1)K_D t)^{1/1-n} \quad n \neq 1 \quad (5)$$

with $R_p = (R_{p,0}^{(1-n)} + (n-1)K_D t)^{1/1-n}$

For each experiment, the determined reaction rates have been fitted to this equation. Figure 1 shows the typical shape of the reaction rate curves obtained in the experiments. After an induction period of a few minutes, in which the catalyst is activated by the cocatalyst, the catalyst reaches its highest activity and after that follows a typical Ziegler–Natta decay behavior. In the simulations, we have neglected the induction period and used only the experimental data *after* the maximum activity ($R_{p,max}$) to fit eq. (5). The values obtained for the initial reaction rate ($R_{p,0}$) and the deactivation constant (K_D) have been used to analyze the various process parameters in a qualitative and quantitative manner. For each process parameter varied, we have studied the influence on the yield, maximum reaction rate, deactivation rate, and induction period as follows.

Influence of Hydrogen

In almost every commercial olefin polymerization, hydrogen is used as a chain transfer agent to regulate the molecular weight of the polymer. Several authors have reported hydrogen also influences the reaction rate and the decay behavior of the catalyst; see Barbé et al.[2] and Albizatti et al.[1] We have investigated the influence of hydrogen on the integral yield, maximum rate, deactivation constant, and the induction period in a series of experiments with hydrogen concentrations in the gas cap from 0.0 to 12.1 vol. % of the reactor. In the experimental series all process conditions have been kept constant, see Table I,

Table I. Process Parameters for the Various Experimental Series with Each Experiment Executed with 30 mg of $MgCl_2/TiCl_4/EB$ Catalyst at a Temperature of 42°C for 75 min

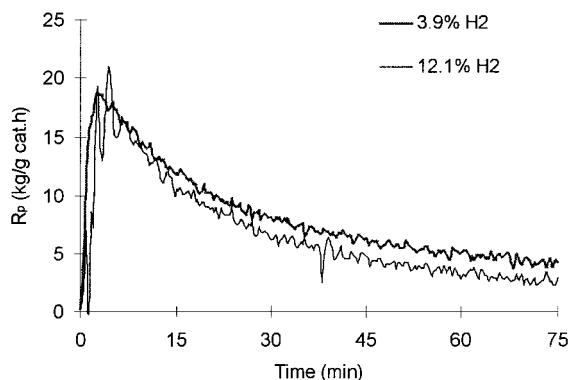| Variable	[H₂] (vol. %)	TEA1 (mg)	PEEB (mg)	$r_{TEAl/Ti}$ (−)	$r_{PEEB/TEAl}$ (−)
[H₂]	0–12	250	215	116	0.5
$r_{TEAl/Ti}$	4	250–1000	215–1720	100–900	0.5
$r_{PEEB/TEAl}$	4	250	0–464	116	0–2

Figure 2. Reaction rate curves of two experiments executed with hydrogen concentrations of 3.9% and 12.1%.

except for the hydrogen concentration.

Figure 1 shows the reaction rate curves for no hydrogen and a hydrogen concentration of 3.9%. The reaction rate for no hydrogen reaches a maximum of 10 kg/(g of catal. h) after about 5 min and after that slowly decays. In the presence of a moderate hydrogen concentration in the gas cap of 3.9%, a much higher maximum reaction rate is reached after 3 min, but the deactivation rate is also significantly faster. In the final stage of the reaction, the remaining activity is at about the same level for both experiments.

Figure 2 shows the reaction rates for hydrogen concentrations of 3.9% and 12.1%. The maximum reaction rate and the induction period are almost the same in both cases, but the deactivation is faster for the higher hydrogen concentration.

In Figure 3a, the yield is given as a function of the hydrogen concentration. Remarkable is the large increase in yield when a small amount of hydrogen is added to the reactor. Compared to the case for the absence of hydrogen, the yield almost doubles at a hydrogen concentration of 2%. Above this concentration the yield decreases slightly.

Figure 3b shows a plot of the measured maximum reaction rate versus the hydrogen concentration. The maximum strongly increases in the low concentration range of hydrogen. For concentrations above 2%, the maximum reaches a constant value of about 16 kg/(g of catal. h).

Figure 3c shows the deactivation constant increases linearly with increasing hydrogen concentration. Figure 3d shows the induction period is shortened from 5 to 3 min with increasing hydrogen concentration in the lower concentrations range and beyond that remains constant.

The experimental results given above illustrate the strong influence of hydrogen on the po-

lymerization rate. Polymerization with a few percent of hydrogen results in a doubling of the yield and the maximum rate. This strong increase in catalyst activity most likely is a result of the reactivation of the sites that have been deactivated by a regioirregular 2,1 insertion; see Figure 4. After a 1,2 insertion of propylene the center is still active, while for the 2,1 insertion an activated site remains in an inactive, "dormant" state due to the steric hindrance of the methyl group close to the Ti atom. The reactivation by hydrogen will be further discussed in the next paragraph. The observed increase in deactivation rate with increasing hydrogen concentrations may be explained by a deactivation reaction between the Ti—H bond and the carbonyl group of the ester; see Albizatti et al.[1] With increasing hydrogen concentrations, the concentration of the relatively unstable Ti—H active centers also increases and so does the deactivation rate.

Hydrogen Reactivation Effect

To investigate the hydrogen reactivation effect, two experiments have been executed with a high and a low PEEB concentration. The initial hydrogen concentration in the gas cap is about 0.3%, and after 60 min, the hydrogen concentration quickly has been raised to 12%. In a third experiment the reactor pressure has been increased with nitrogen from 27 to 36 bar after 30 min to verify whether the hydrogen causes the reactivation. Figure 5 shows the reaction rate curves at a low and a high concentration of PEEB. At the low PEEB concentration, the reaction rate immediately increases more than 40% after increasing the hydrogen concentration; at the high PEEB concentration, the reaction rate increases about 10–20% after increasing the hydrogen concentration.

Figure 6 shows the reaction rate curve of the third experiment executed at 57°C with a hydrogen concentration of 4%. After 30 min, the reactor pressure is increased with nitrogen from 27 to 36 bar. This does not influence the rate curve at all and proves the observed increase of the catalyst activity indeed is a result of the increase in hydrogen concentration rather than of an increased reactor pressure.

Several authors have reported about this reactivation effect by hydrogen; see Bukatov et al.[3] and Busico et al.[4] Bukatov[3] observes the reactivation is confined to propylene polymerizations; in the case of ethylene polymerizations in the presence of hydrogen, no increase of the reaction
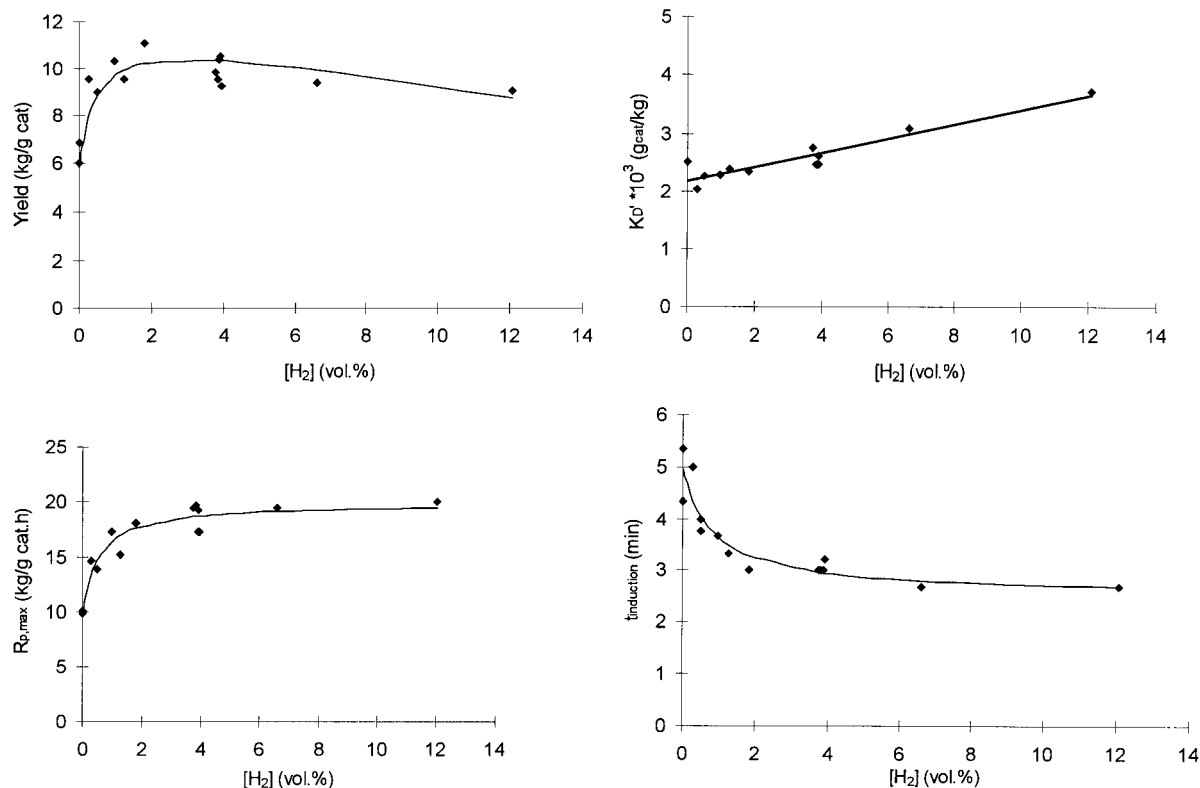
Figure 3. Influence of the hydrogen concentration, at the standard TEA1/Ti and PEEB/TEA1 molar ratio, on the following: (a) yield after a reaction time of 75 min; (b) maximum reaction rate $R_{p,max}$; (c) deactivation constant K'_d; (d) induction period t_i.

rate has been observed. He suggests the reactivation may be a result of the presence of two different types of active centers. The first type is less stereospecific and inserts propylene via the regular 1,2 insertion and irregular 2,1 insertions; the second is highly stereospecific and deactivates to a dormant center after a regioirregular 2,1 insertion; see Figure 4. Chain transfer with hydrogen may reactivate the dormant centers; see Spitz et al.[9,10] and Guyot et al.[6] This hypothesis is supported by the presence of n-butyl chain end groups in polymers synthesized in the presence of hydrogen; see Chadwick et al.[5] Another possibil-
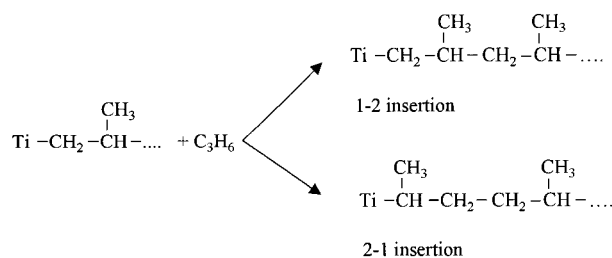
ity is hydrogen reacts with the dormant centers to form active Ti–propyl centers. The reason for the much higher activation at lower PEEB concentrations probably is that PEEB is involved in the irreversible deactivation of the dormant sites. Increasing the hydrogen concentration in a later stage of the reaction, therefore, has a much stron-
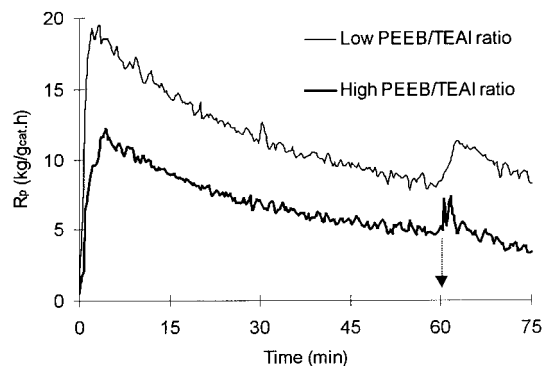

Figure 4. Regioregular 1,2 and regioirregular 2,1 insertion of propylene.

Figure 5. Reaction rate curves at a low and a high PEEB/TEAl molar ratio. After 60 min the hydrogen concentration has been increased from 0.27 vol. % to 12 vol. %.
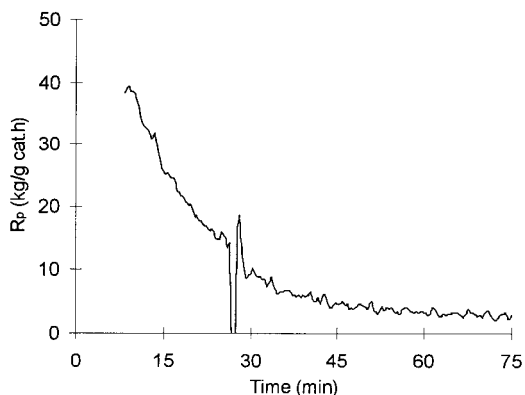
Figure 6. Reaction rate curve of an experiment where after 26 min the reactor pressure has been increased with nitrogen from 26 to 35 bar.

ger effect at low PEEB concentrations where the deactivation rate of the dormant sites has been slower.

The influence of hydrogen on the induction period is significant. From a hydrogen concentration of 0.0% up to 2%, the induction period decreases from 5 to 3 min. This indicates hydrogen enhances the initiation of the reaction.

Above hydrogen concentrations of 2% initiation is no further enhanced, probably because another step in the formation of active centers becomes limiting.

Influence of the PEEB/TEAl Ratio at a Constant TEAl/Ti Ratio

The influence of the electron donor on the reaction rate curve has been studied by varying the PEEB/TEAl ratio at the standard hydrogen concentration and TEAl/PEEB molar ratio; see Table 1.

Figure 7a shows the polymer yield decreases strongly with an increasing PEEB/TEAl ratio. Without PEEB, an extraordinary high yield has been obtained, but the polymer produced formed a sticky, waxy clump that completely plugged the reactor: a typical result for polymers with a very low isotacticity. At a PEEB/TEAl ratio of 0.15 the yield decreases by 30% but the product obtained is a dry, free flowing powder. This points to a much higher isotacticity of the polymer than without PEEB. With an increasing PEEB/TEAl ratio up to a value of 0.75, the yield progressively decreases. Above a ratio of 1, the catalyst has completely lost its activity.
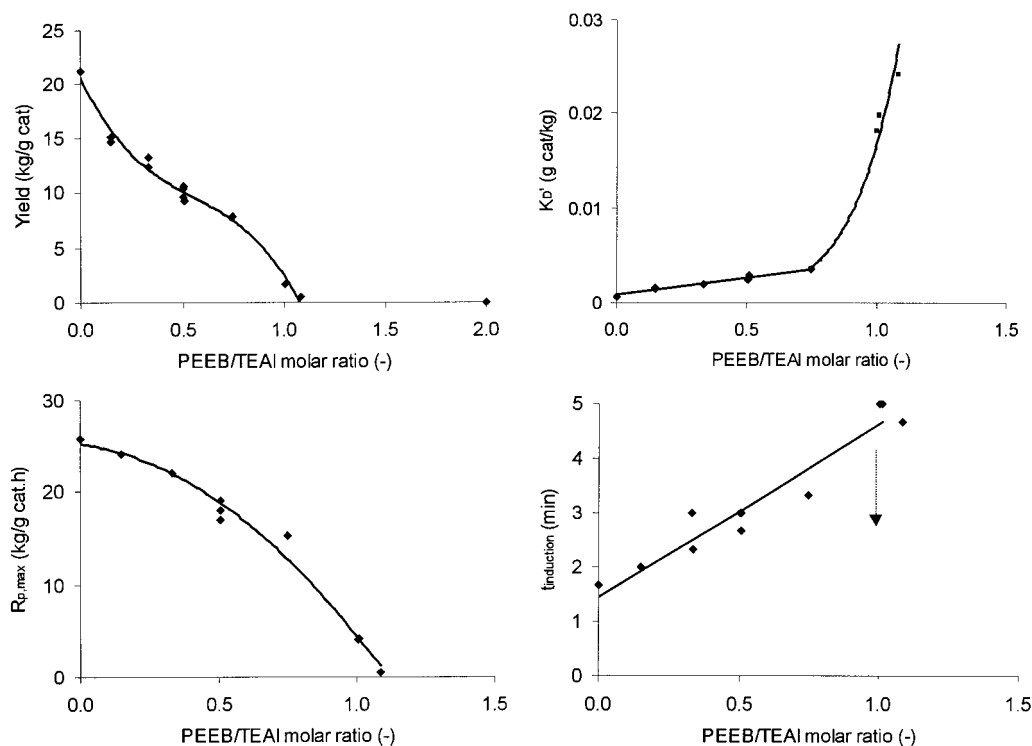

Figure 7. Influence of the PEEB/TEAl molar ratio, at a hydrogen concentration of 4 vol. % and a TEAl/Ti ratio of 116, on the following: (a) yield after 75 min of reaction time; (b) maximum reaction rate $R_{p,max}$; (c) deactivation constant K_D; (d) induction period t_i.
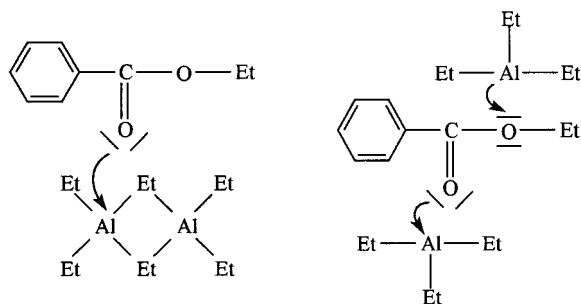
Figure 8. Proposed configurations of the PEEB/TEAl complex in a 1 : 2 ratio.

In Figure 7b, the maximum reaction rate is given as a function of the PEEB/TEAl ratio. This figure shows the maximum reaction rate decreases about 25% compared to the maximum reaction rate without PEEB, when the PEEB/TEAl ratio is increased from 0.0 to 0.5; at a PEEB/TEAl ratio of 0.75 it is decreased already to about 40% of the maximum rate without PEEB. Further increase of the PEEB/TEAl ratio leads to a rate zero at a ratio of around 1.0.

Figure 7c shows the deactivation constant increases with an increasing PEEB/TEAl ratio, first slowly and later rapidly above a ratio of 0.75. Figure 7d shows the induction period as a function of the ratio PEEB/TEAl. The induction period increases linearly from 1.5 to 5 min in the experimental range, and above a PEEB/TEAl ratio of 1, the reaction suddenly stops.

The effect of the electron donor depends on the nature of the electron donor and the catalyst system used. Our experimental results are in agreement with earlier published investigations with MgCl$_2$/TiCl$_4$/ethyl benzoate–TEAl catalyst systems.[2] The use of an electron donor leads to a significant increase in stereospecificity and a drastic decrease in catalyst yield. The role of the electron donor is believed to be 2-fold. The electron donor probably poisons selectively a great part of the atactic sites, which also explains the decrease in catalyst activity. Second, the electron donor probably modifies the remaining active sites to highly stereospecific centers. So, the increase in isotactic polymer yield is attributed to the transformation of a part of the atactic sites to isospecific sites.

The observed decrease in yield with an increasing PEEB/TEAl ratio is a result of the above described decreasing maximum yield and increasing deactivation. The effect of the electron donor on the catalyst activity can be explained by the reaction mechanism proposed by Spitz.[11] He sug-

gests that the electron donor and the cocatalyst may form two types of complexes. The first type is a complex with an electron donor/cocatalyst ratio of 1 : 2; see Figure 8. This complex is responsible for the modification of active sites into highly specific sites which is supported by our investigations. At an electron donor/cocatalyst ratio of 1 : 2, the yield is still 60% of the yield obtained without PEEB, while the quality of the polymer powder produced is good.

The second type is a complex with an electron donor/cocatalyst ratio of 1 : 1, as is illustrated in Figure 9. In the presence of this complex, the catalyst deactivates completely. This implies the 1 : 1 electron donor/cocatalyst complex blocks all available active centers. This also may explain the very strong increase of the deactivation constant observed above a PEEB/TEAl ratio of 0.5, where the formation of the 1 : 1 electron donor/cocatalyst complex starts, as shown in Figure 7c. For an electron donor/cocatalyst ratio of 1 and higher, the reaction rate is zero.

The increase of the induction period with increasing PEEB/TEAl ratios points to a formation of active centers with a complex of cocatalyst and electron donor, much slower than the formation of active centers without electron donor. This delay may be explained by the large size of the complex of the electron donor and cocatalyst, which makes a transfer to the active centers and a following activation much more difficult.

Influence of the TEAl/Ti Ratio at a Constant PEEB/TEAl Ratio

In the next series of experiments, the influence of the molar ratio of cocatalyst and catalyst on the reaction rate curve has been studied at the standard hydrogen concentration and PEEB/TEAl molar ratio; see Table I. This implies a proportional change of the concentrations of cocatalyst and electron donor in the reactor.

Figure 10a shows the yield is almost independent of the TEAl/Ti ratio. For a TEAl/Ti ratio of
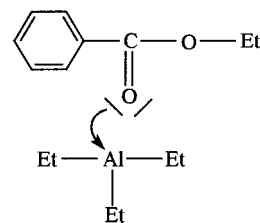

Figure 9. Proposed configuration of the PEEB/TEAl complex in a 1 : 1 ratio.
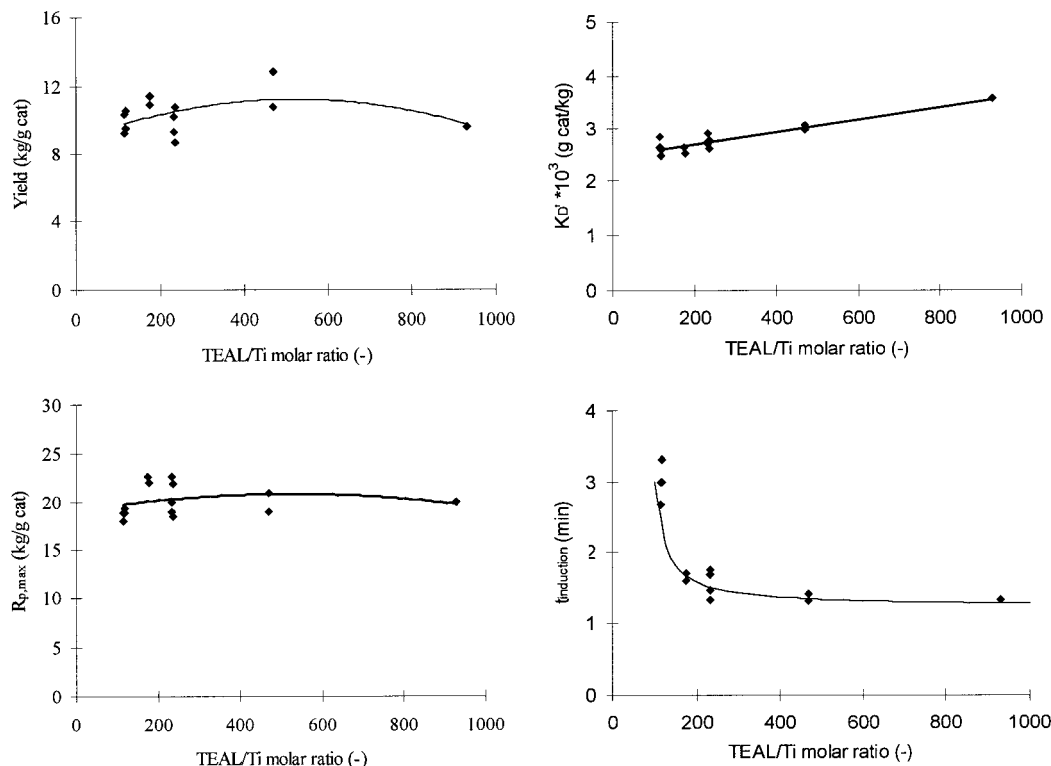
Figure 10. Influence of the TEAl/Ti molar ratio, at a hydrogen concentration of 4 vol. % and a PEEB/TEAl ratio of 2.0, on the following: (a) yield after 75 min of reaction time; (b) maximum reaction rate $R_{p,max}$; (c) deactivation constant K_D; (d) induction period t_i.

100–500, a slight increase in yield is observed, and above 500, a slow decrease is observed. Figure 10b shows the maximum reaction rate ($R_{p,max}$) is also almost independent of the TEAl/Ti ratio. Also here a hardly noticeable maximum for the maximum reaction rate is found for a TEAl/Ti ratio of 500. Figure 10c shows the deactivation constant K_D increases slowly but significantly with an increasing TEAl/Ti ratio. In Figure 10d the induction period strongly decreases, from 3.5 to 1.5, when the TEAl/Ti ratio increases from 100 to 200. Above a TEAl/PEEB ratio of 200, the induction period remains constant at about 1.3 min.

The results given above show there is a small influence of the ratio of TEAl/Ti; at a TEAl/Ti ratio of about 500, a maximum yield is obtained. As long as the PEEB/TEAl ratio is maintained constant, the influence of their concentration on the reaction rate is minimal. Similar results have been reported by Barbé et al.[2] for the same type of catalyst. Keii (Keii et al., 1982) executed his experiments at much lower TEAl/Ti ratios, from about 0.2 to 5, and found a strong influence of the concentration of TEAl. He also observed a weak maximum in activity with increasing TEAl con-

centrations. As our experiments are executed at much higher TEAl/Ti ratios of > 100, all sites have been activated already. Remarkable is the stability in kinetics, even at very high TEAl/Ti ratios. This indicates the alkylation reaction between TEAl and PEEB, of which the reaction products may deactivate the catalyst, is still negligible at a temperature of 42°C.

The observed decrease of the induction period from 3.5 to 1.5 min, when the TEAl/Ti ratio is increased from 100 to 250, is attributed to a faster activation of the active centers due a faster transfer of the cocatalyst to the active centers. Above that ratio, the induction period becomes constant, probably because the formation of the active complex now becomes the limiting step.

MODELING

The reaction rates have been modeled at isothermal conditions as a function of the hydrogen concentration and the molar ratios of TEAl/Ti and PEEB/TEAl. In the experiments described earlier in this article, we have varied one of the three

Table II. Standard Values and Validity Intervals of Parameters of the Model

Variable	Standard Value	Validity Interval
$[H_2]$ (vol. %)	4	0–12
$r_{TEAl/Ti}$ (−)	116	100–900
$r_{PEEB/TEAl}$ (−)	0.5	0–0.75

said parameters systematically while keeping the two others at a constant, standard value. For each experiment, the reaction rates have been fitted to the kinetic model, eq. (5), which is also given below:

$$R_p = (R_{p,0}^{(1-n)} + (n-1)K_D t)^{1/1-n} \quad (5)$$

From the experiments described earlier, we have learned that under isothermal conditions, the initial reaction rate $R_{p,0}$ and the deactivation constant K_D' can be described as functions of three parameters:

$$R_{p,0} = f([H_2], r_{TEAl/Ti}, r_{PEEB/TEAl}) \quad (6)$$

$$K_D' = G([H_2], r_{TEAl/Ti}, r_{PEEB/TEAl}) \quad (7)$$

where $r_{TEAl/Ti}$ and $r_{PEEB/TEAl}$ are the TEAl/Ti and PEEB/TEAl molar ratios, respectively. Table II shows the hydrogen concentration and the TEAl/Ti and PEEB/TEAl ratios of the standard experiment together with the interval in which these parameters have been modeled. First, we will describe the influence of each of the before mentioned parameters on $R_{p,0}$ and K_D' when the other two parameters are kept at the standard values. This is followed by an overall model, in which the reaction rate is presented as a function of the hydrogen concentration *and* the TEAl/Ti and PEEB/TEAl molar ratios.

Modeling of the Reaction Rate as a Function of the Hydrogen Concentration

The influence of the hydrogen concentration on the reaction rate has been modeled at the standard molar ratios of TEAl/Ti and PEEB/TEAl using the $R_{p,0}$ and K_D' values obtained from the best fit of the experimental data to the kinetic model. Figure 11 shows the initial reaction rate increases with increasing hydrogen concentration up to a hydrogen concentration of about 4%. Above this concentration the initial rate reaches an asymp-

totic maximum, which indicates the hydrogen concentration decreases the lifetime of the dormant sites and their quasi steady-state concentration. We have described $R_{p,0}$ as a function of the hydrogen concentration on the basis of the following assumptions:

- Initially, two types of sites can be distinguished: one type is active, and the other has been transformed into an inactive, "dormant" site by regioirregular 2,1 insertion. The third site type, the irreversibly deactivated site, is neglected in the very beginning of the reaction.
- The reactivation rate of dormant sites is first order in the hydrogen concentration.
- The reaction rate is proportional to the total concentration of active centers and the reactivity of the different site types is the same.
- The reaction rate is a function of the TEAl/Ti and PEEB/TEAl molar ratios, rather than a function of the individual concentration of these components.

The following population balance gives the number of polymerizing active sites:

$$P^* = P_t^* - P_D^* \quad (8)$$

Here P^* is the concentration of polymerizing sites, P_t^* is the total concentration of both the active and the dormant sites, and P_D^* is the concentration of the dormant sites.

The various propagation and reactivation reactions occurring at the active and dormant sites, respectively, are described as follows:
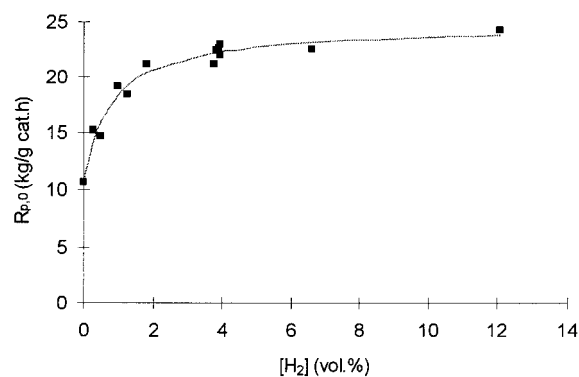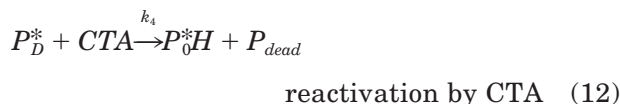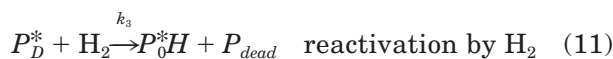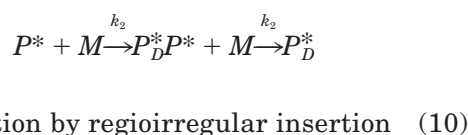

Figure 11. Fitted initial reaction rate $R_{p,0}$ as a function of the hydrogen concentration at a TEAl/Ti ratio of 116 and a PEEB/TEAl ratio of 0.5.

Table III. Standard Values of the Initial Reaction Rate $R_{p,0}(st.)$ and the Deactivation Constant $K_D'(st.)$ and the Values of the Overall Model Parameters a_1–a_{14}

$R_{p,0}(st.) \ = \ 22.3$ kg/(g of catal. h)	$K_D'(st.) \ = \ 2.7 \ \times \ 10^{-3}$ g of catal./kg
$a_1 \ = \ 0.63$	$a_8 \ = \ 4.44 \times 10^{-4}$
$a_2 \ = \ 1.22$	$a_9 \ = \ 0.91$
$a_3 \ = \ 1.11$	$a_{10} \ = \ -1.42$
$a_4 \ = \ 0.045$	$a_{11} \ = \ 0.58$
$a_5 \ = \ 0.81$	$a_{12} \ = \ 1.11$
$a_6 \ = \ 2.34 \times 10^{-4}$	$a_{13} \ = \ 1.37$
$a_7 \ = \ 0.93$	$a_{14} \ = \ 0.296$

$$P* + M \xrightarrow{k_1} P* \quad \text{propagation} \tag{9}$$

$$P* + M \xrightarrow{k_2} P_D^* \quad P* + M \xrightarrow{k_2} P_D^*$$

deactivation by regioirregular insertion   (10)

$$P_D^* + H_2 \xrightarrow{k_3} P_0^* H + P_{dead} \quad \text{reactivation by H}_2 \tag{11}$$

$$P_D^* + CTA \xrightarrow{k_4} P_0^* H + P_{dead}$$

reactivation by CTA   (12)

Here $P_0^* H$ is an active site without polymer, P_D^* is a dormant center, P_{dead} is a dead polymer, and CTA is any chain transfer agent other than H_2. The reaction rate is given by the following equation:

$$R_{p,0} = k_p P*[M] \tag{13}$$

With the quasi steady-state assumption for the formation and reactivation of dormant sites, combination of eqs. 10–12 gives

$$R_D = k_2 P* M - k_3 P_D^*[H_2] - k_4 P_D^*[CTA] = 0 \tag{14}$$

$$P_D^* = \frac{k_2'}{k_1'[H_2] + 1} \tag{15}$$

with $k_1' \ = \ k_3/(k_4[CTA])$ and $k_2' \ = \ k_2 P* M/(k_4[CTA])$.

Combination of the eqs. 8 and 15 gives the concentration of active sites as a function of the hydrogen concentration:

$$P* = P_t^* - \frac{k_2'}{k_1'[H_2] + 1} \tag{16}$$

Furthermore, we define the variable f_{H_2} as the factor by which the initial rate at standard conditions, $R_{p,0}(st.)$, has to be multiplied to obtain the $R_{p,0}$ value at any given hydrogen concentration:

$$f_{H_2} = \frac{R_{p,0}}{R_{p,0}(st.)} \tag{17}$$

Combination of the eqs. 13, 16, and 17 gives

$$f_{H_2} = a_3 - \frac{a_1}{1 + a_2[H_2]} \tag{18}$$

The constants a_1–a_3 have been calculated on the basis of the data in Figure 11 and the initial reaction rate at standard conditions. The values of these constants are given in Table III.

K_D' has been found to be a linear function of the hydrogen concentration, see Figure 3c, and has been described as such:

$$K_D' = a_4'[H_2] + a_5' \tag{19}$$

The factor by which the deactivation constant at standard conditions, $K_D'(st.)$, has to be multiplied to obtain K_D' at a given hydrogen concentration is given by the following equation:

$$g_{H_2} = \frac{K_D'}{K_D'(st.)} \tag{20}$$

Combination of the eqs. 19 and 20 gives

$$g_{H_2} = a_4[H_2] + a_5 \tag{21}$$

The constants a_4 and a_5 have been calculated on the basis of the data in Figure 3c and the deactivation constant at standard conditions. The values of these constants are given in Table III.

Modeling of the Reaction Rate as a Function of the TEAl/Ti Ratio

The influence of the TEAl/Ti ratio on the reaction rate has been modeled at the standard hydrogen concentration and PEEB/TEAl ratio, using the $R_{p,0}$ and K'_d values obtained from the best fit to the experimental data. Analogous to the model given above, the $R_{p,0}$ and K'_D values have been described as a function of the TEAl/Ti ratio. The factor by which the standard initial reaction rate has to be multiplied to obtain the initial reaction rate at a given TEAl/Ti ratio has been defined as

$$f_{TEAl/Ti} = R_{p,0}/R_{p,0}(st) \qquad (22)$$

As the reaction rate has been found to be a linear function of the TEAl/Ti ratio, it has been described by the following equation:

$$f_{TEAl/Ti} = a_6 r_{TEAl/Ti} + a_7 \qquad (23)$$

The factor by which the standard deactivation constant has to be multiplied to obtain the actual deactivation constant at a given TEAl/Ti ratio has been defined as follows:

$$g_{TEAl/Ti} = \frac{K'_D}{K'_D(st.)} \qquad (24)$$

As the deactivation constant has been found to be a linear function of the TEAl/Ti ratio, it has been described with the following equation:

$$g_{TEAl/Ti} = a_8 r_{TEAl/Ti} + a_9 \qquad (25)$$

The values of the constants a_6–a_9 are given in Table III.

Modeling of the Reaction Rate as a Function of the PEEB/TEAl Ratio

The reaction rate has been modeled as a function of the PEEB/TEAl ratio at the standard hydrogen concentration and TEAl/Ti ratio. The $R_{p,0}$ and K'_d values obtained from the best fit to the experimental data have been described as a function of the PEEB/TEAl ratio, whereas $f_{PEEB/TEAl}$ and

$g_{PEEB/TEAl}$ have been defined and described in a similar way as above:

$$f_{PEEB/TEAl} = a_{10} r^2_{PEEB/TEA} + a_{11} r_{PEEB/TEAl} + a_{12} \qquad (26)$$

$$g_{PEEB/TEAl} = a_{13} r_{PEEB/TEAl} + a_{14} \qquad (27)$$

The values of the constants a_{10}–a_{14} have been calculated on the basis of the experimental data and are given in Table III.

Overall Model

The overall model is based on the simplifying assumption that the hydrogen concentration, the TEAl/Ti ratio, and the PEEB/TEAl ratio influence the reaction rate independently of each other. Therefore, the initial reaction rate and the deactivation constant have been described as follows:

$$R_{p,0} = R_{p,0}(st.) f_{H_2} f_{TEAl/Ti} f_{PEEB/TEAl} \qquad (28)$$

$$K_D = K_D(st.) g_{H_2} g_{TEAl/Ti} g_{PEEB/TEAl} \qquad (29)$$

Validation of the Overall Model

To validate the model, the experimental reaction rates have been compared with the modeled reaction rates for experiments where only one parameter has been varied from its standard value as well as for experiments where more than one parameter have been varied at the same time. In both cases the agreement between the experiment and the model is rather good. In Figure 12a–d the experimental and calculated reaction rate curves are shown for experiments where more than one of the parameters have been varied from the standard value. Figure 12a,b shows the model describes the experimental data rather well, even if the hydrogen concentration as well as the TEAl/Ti and PEEB/TEAl molar ratios are varied significantly. Figure 12c,d show the model describes the experimental curves not as well as in Figure 12a,b but still reasonable at very low hydrogen concentrations and varying PEEB/TEAl ratios. The deviation between the model and the experiment becomes larger for the lower hydrogen concentrations, because small errors in the amount of hydrogen fed into the reactor introduce relatively large errors in the estimated initial rate values. The reason for this is the initial reaction rate increases strongly with in-
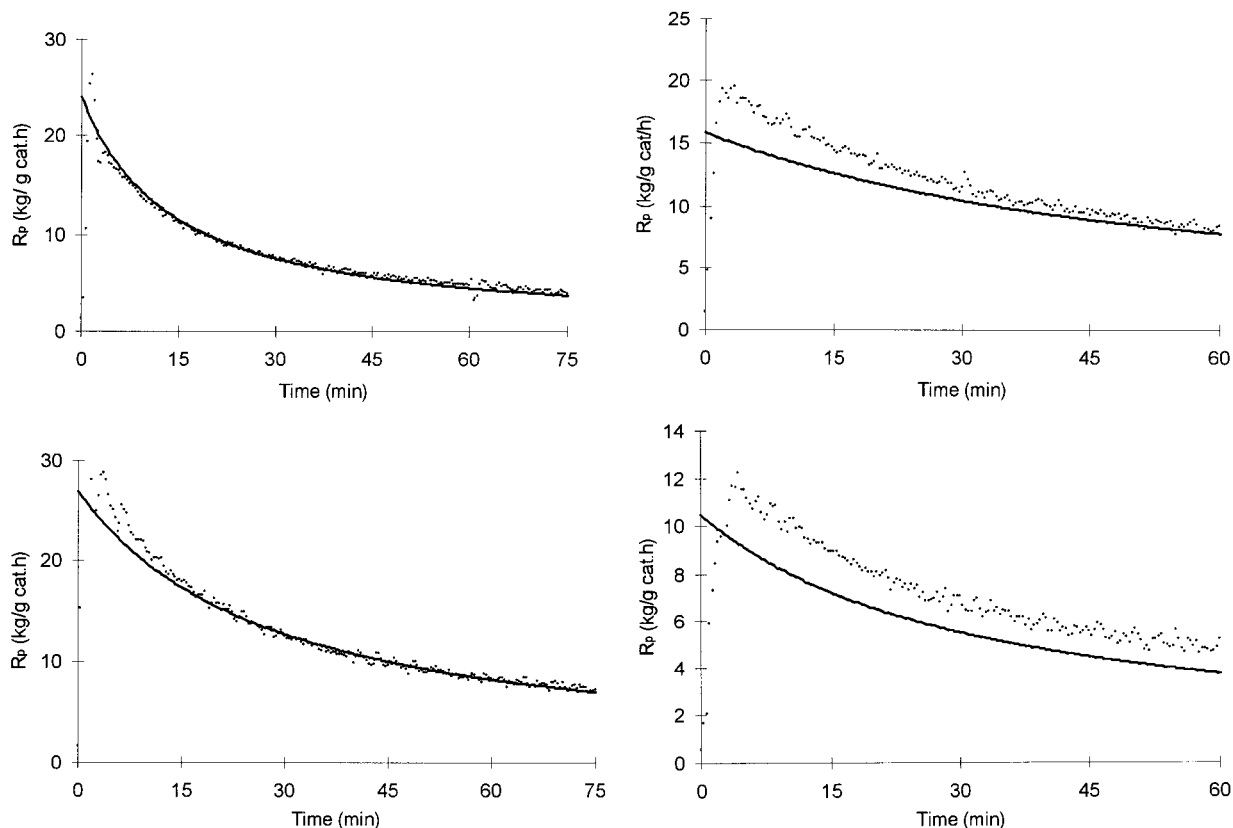
Figure 12. Experimental and calculated reaction rate curves where at the same time more than one of the parameters $[H_2]$, $r_{TEAl/Ti}$, and $r_{PEEB/TEAl}$ have been changed from their standard values: (a) $[H_2] = 2[H_2](st.)$, $r_{TEAl/Ti} = 2r_{TEAl/Ti}(st.)$, $r_{TEAl/Ti} = 0.5r_{PEEBTEAl}$; (b) $[H_2] = [H_2](st.)$, $r_{TEAl/Ti} = 4r_{TEAl/Ti}(st.)$, $r_{TEAl/Ti} = 0.25r_{PEEBTEAl}$; (c) $[H_2] = 0.07[H_2](st.)$, $r_{TEAl/Ti} = 2r_{TEAl/Ti}(st.)$, $r_{TEAl/Ti} = 0.5r_{PEEBTEAl}$; (d) $[H_2] = 0.08[H_2](st.)$, $r_{TEAl/Ti} = r_{TEAl/Ti}(st.)$, $r_{TEAl/Ti} = 1.5r_{PEEBTEAl}$.

creasing hydrogen concentration at low hydrogen concentrations, as has been shown in Figure 11.

Model Simulations

The model has been used to illustrate the influence of the most important variables, i.e. the hydrogen concentration and the PEEB/TEAl ratio, on the reaction rate curves. Figure 13 shows the calculated rate curves for different hydrogen concentrations. Remarkably the reaction rates obtained with hydrogen seem to approach those obtained without hydrogen in the final stage. This indicates the reactivation effect by hydrogen is extinguished, which is believed to be a result of the deactivation after the chain transfer with hydrogen of the relatively unstable Ti—H sites rather than a result of depletion of hydrogen; see Spitz.[9] Only at low hydrogen concentrations depletion of hydrogen may occur. The increase in

the deactivation rate with increasing hydrogen concentration probably is a result of an increasing rate of the chain transfer with hydrogen and with
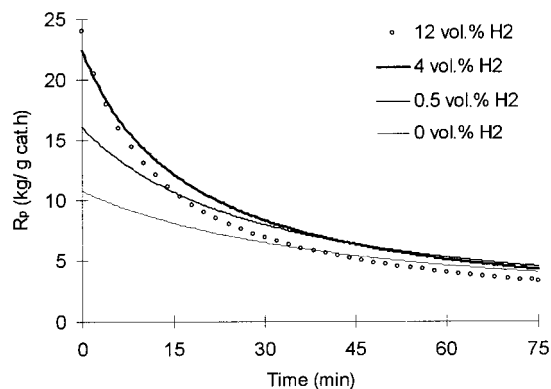

Figure 13. Calculated reaction rate curves as a function of the hydrogen concentration whereas the other parameters are kept constant: $r_{PEEB/TEAl} = 0.5$; $r_{TEAl/Ti} = 120$; $T = 42°C$.
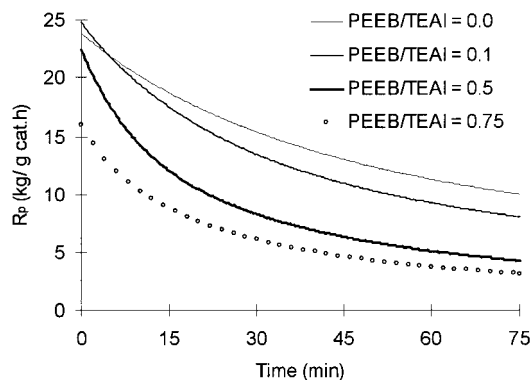
Figure 14. Calculated reaction rate curves as a function of $r_{PEEB/TEAl}$ whereas the other parameters are kept constant: $H_2 = 4\%$; $r_{TEAl/Ti} = 120$; $T = 42°C$.

that an increase in the concentration of unstable Ti—H sites.

The influence of the PEEB/TEAl ratio on the reaction rate is illustrated in Figure 14, showing that, up to a PEEB/TEAl ratio of 0.5, the initial reaction rate is rather independent of the PEEB/TEAl ratio, while the deactivation rate increases with an increasing PEEB/TEAl ratio. Above a PEEB/TEAl ratio of 0.5 the initial rate decreases, which indicates a deactivation of the sites by the 1 : 1 PEEB/TEAl complex or free PEEB in the very beginning.

CONCLUSIONS

We have proven the suitability of liquid pool propylene polymerization on a small scale to investigate reaction kinetics, in this case the activity and decay behavior of a highly active $MgCl_2/TiCl_4/EB$ catalyst as a function of the process conditions. The kinetics have been described by means of a relatively simple kinetic model with the initial reaction rate and deactivation constant as the key variables. The major results of our experimental investigations with the above type of catalyst are summarized below.

The presence of hydrogen strongly increases the initial activity of the catalyst; this is attributed to a reactivation of dormant sites by hydrogen. At the same time the deactivation rate increases significantly with increasing hydrogen concentrations. At about 2% hydrogen an optimum yield, twice as high as without hydrogen, is obtained. Furthermore, the presence of hydrogen decreases the induction period significantly, indicating hydrogen stimulates the initiation of the reaction.

The PEEB/TEAl ratio has a strong impact on the catalyst activity and decay. Polymerization without PEEB results in a very high initial activity followed by a slow deactivation rate. However, in the presence of PEEB—already at low PEEB/TEAl ratios—the isotacticity improves significantly. Above a PEEB/TEAl ratio of 0.5 the catalyst activity decreases quickly with an increasing PEEB/TEAl ratio. Above a PEEB/TEAl ratio of 1, no propagation takes place anymore. Furthermore, the presence of PEEB seems to delay the initiation of the propagation, because the induction period increases significantly in the presence of PEEB.

The TEAl/Ti ratio has a relatively small influence on the catalyst activity and the decay rate as long as this ratio is above about 100 and the PEEB/TEAl ratio is maintained constant. This implies the greater part of the potentially active centers is already activated at TEAl/Ti ratios of about 100 and the TEAl/PEEB complex does not obstruct the adsorption of monomer at the active centers, even at higher concentrations of the TEAl and PEEB.

Finally, we have presented an empirical model which describes the experimental rate curves as a function of the hydrogen concentration and the TEAl/Ti and PEEB/TEAl ratios rather well. Model calculations show the hydrogen reactivation effect is extinguished, probably as a result of irreversible deactivation of the Ti—H complex. Furthermore, the deactivation rate increases with an increasing PEEB/TEAl ratio. The initial reaction rate is rather constant for PEEB/TEAl ratios up to 0.5; above this ratio the initial reaction rate decreases.

As the performance of a catalyst system depends strongly on the combination of the catalyst, cocatalyst, and the internal and external electron donors, our experimental data and model should be applied with care. For a similar catalyst system, the exact activities and deactivation rate may vary, but the trends should be comparable; for a different combination of catalyst, cocatalyst, and electron donors, the results are probably not usable. However, a similar approach could be applied to investigate other catalyst systems to describe the rather complex kinetics in a manageable way.

The properties of polymers produced in the liquid as well as in the gas phase with the catalyst system used in this work will be compared in our further work. The kinetic data will be used in an experimental study of a small fluidized bed reactor for olefin polymerizations.

NOTATION

a_1–a_{14}	constants
C_m	monomer concentration (kg/m^3)
C^*	number of active sites per gram of catalyst, mol/g of catal.
E_a	activation energy (kJ/mol)
f	reaction rate divided by the rate at standard conditions ($-$)
g	deactivation constant divided by the deactivation constant at standard conditions ($-$)
g of catal.	gram MgCl$_2$/TiCl$_4$/EB catalyst (g)
[H$_2$]	hydrogen concentration (vol. %)
k_d	deactivation constant, for 2nd-order deactivation, [(mol of active centers/g of catal.) h^{-1}]
K_D	overall deactivation constant, for 2nd-order (g of catal. m^{-3})
K'_D	K_D/C_m (g of catal./kg)
$K'_D(st.)$	deactivation constant at standard conditions (g of catal./kg)
k_p	propagation reaction constant [m^3/(mol of active centers h)]
k_1–k_4	kinetic constants
n	order of deactivation ($-$)
P_t^*	total concentration of both active and dormant centers (mol/g of catal.)
P^*	concentration polymerizing sites (mol/g of catal.)
P_D^*	dormant sites (mol/g of catal.)
P_{dead}	dead polymer
$r_{TEAl/PEEB}$	molar ratio of TEAl and PEEB ($-$)
$r_{TEAl/PEEB}$	molar ratio of TEAl and PEEB ($-$)
R	gas constant [J/(mol K)]
R_D	deactivation rate to dormant sites (mol sites/g of catal.)
R_p	polymerization rate [kg/(g of catal. h)]
$R_{p,0}$	initial polymerization rate [kg/(g of catal. h)]
$R_{p,0}(st.)$	initial reaction rate at standard conditions, kg/g catal. of h
$R_{p,max}$	maximum reaction rate [kg/(g of catal. h)]
t	time (h)
T	temperature (K)
Y	yield (kg/g of catal.)

Subscripts

catal.	catalyst
i	induction, induction period
L	liquid phase
m	monomer
p	polymerization, propagation
PP	polypropylene

Abbreviations

CTA	chain transfer agent
DEAC	diethylaluminum chloride
PEEB	ethyl *p*-ethoxybenzoate
TEA	triethylaluminum

REFERENCES AND NOTES

1. Albizatti, E.; Gianinni, U.; Collina, G.; Noristi, L.; Resconi, L. in Polypropylene handbook; Moore, E. G., Ed.; Carl Hanser Verlag: Munich, Vienna, New York, 1996; chap. 2, p. 74.
2. Barbé, P. C.; Cecchin, G.; Noristi, L. Adv Polym Sci Catal Radical Polym 1987, 81, 3.
3. Bukatov, G. D.; Goncharov, V. S.; Zakharov, V. A.; Dudchenko, V. K.; Sergeev, S. A. Kinet Catal, 1994, 35(3), 358.
4. Busico, V.; Corradini, P.; de Marino, L.; Proto, A.; Macromol Chem 1986, 187, 1115.
5. Chadwick, J. C.; Miedema, A.; Sudmeijer, O. Macromol Chem Phys 1994, 195, 167.
6. Guyot, A.; Spitz, R.; Dassaud, J. P.; Gomez, G. J Mol Catal 1993, 82, 29.
7. Samson, J. J. C.; Weickert, G.; Heerze, A. E.; Westerterp, K. R. AIChE J.
8. Samson, J. J. C.; Weickert, G.; Heerze, A. E.; Westerterp, K. R. AIChE J, to appear.
9. Spitz, R.; Bobichon, C.; Guyot, A. Macromol Chem 1989, 190, 707.
10. Spitz, R.; Masson, P.; Bobichon, C.; Guyot, A. Macromol Chem 1989, 190, 717.
11. Spitz, R.; Lacombe, J. L.; Primet, M. J. J Polym Sci Chem Ed 1984, 22, 2611.